

# Localization induced by opening; why are most eigenmodes localized in chaotic microcavities?

Jung-Wan Ryu<sup>1</sup> and Sang Wook Kim<sup>2\*</sup>

<sup>1</sup>*Department of Physics, Pusan National University, Busan 609-735, South Korea*

<sup>2</sup>*Department of Physics Education, Pusan National University, Busan 609-735, South Korea*

(Dated: June 4, 2018)

We show that localization occurs when a quantum system is opened with large enough amount. This is understood by considering non-Hermitian random matrices, which also reveals the relation between the non-Hermitian degeneracy, called the exceptional point, and such an opening-induced localization. Based upon it we propose a plausible explanation on a long-lasting question, why most modes are found to be localized in open quantum systems with classically chaotic dynamics. Numerical results obtained from the stadium microcavity confirms our proposal.

PACS numbers: 05.45.Mt, 42.55.Sa

Every real quantum system is inevitably open since no information can be extracted from completely closed systems. However, open quantum systems are very different from closed ones. In the mathematical viewpoint, the closed quantum systems are described by usual Hermitian formalism, while the open ones by non-Hermitian formalism [1, 2]. One of the important feature of non-Hermitian Hamiltonian is the existence of an exceptional point (EP), at which two complex eigenvalues coalesce, so do the corresponding eigenstates [3–5]. The topological property of the EP as a square-root-branch point has been well known; The two eigenstates are exchanged with each other once the parameters vary along a closed loop encircling the EP. The EP has been experimentally observed in various open systems such as microwave cavities [6, 7] and optical microcavities [8]. The EPs, ubiquitous in open quantum systems, often have significant and dramatic consequences in various physical phenomena [9].

Statistical properties of spectra of closed quantum systems are important to study quantum chaos which describes the quantum mechanical behavior of classically chaotic systems [10]. It has been found that the so-called random matrix theory (RMT) successfully explains the statistical nature of the spectra of fully-chaotic systems [11]. According to the RMT, the nearest neighbor spacing of eigenenergies exhibits Wigner distribution in chaotic systems, while Poisson distribution in integrable systems. The RMT predicts the eigenstates of fully chaotic systems are delocalized over the entire accessible energy surface in phase space with some fluctuation described by Porter-Thomas distribution and locally look like random superpositions of the plane waves in coordinate space [12, 13]. Different from most of such chaotic states, a few eigenstates appear to be localized around periodic orbits in the semiclassical regime, which is called as scarring [14–16].

Although the localized eigenstates such as scars are less likely to occur in the *closed* quantum systems with classically chaotic dynamics, they have been much more often observed both experimentally and numerically in

the *open* systems [17–20]. In the recent experiments of deformed dielectric microcavities made of the material with a rather lower  $n$ , where  $n$  is the index of refraction, namely  $n < 2$ , the wide range of spectra exhibit even equidistant spacing, the characteristics of strongly localized modes on periodic orbits [8, 21–25]. While this prevailing localization occurring in open systems has been recognized in the field of quantum chaos for a long time, it has not been fully understood yet why it happens. In this work, we propose a plausible answer of the question, “*why are most modes localized in open quantum systems with classically chaotic dynamics?*”, using the non-Hermitian matrix model with random elements. The key idea is that as the opening becomes bigger the imaginary parts of the eigenenergy, the characteristics of open quantum systems, of the localized modes dominate the coupling or the mixing among the modes so that each mode is decoupled from the others to be localized. We show this is directly related to the EP of a simple  $2 \times 2$  matrix model, and straightforwardly extended to more general cases.

In order to study the effect of opening in a quantum system, we consider the non-Hermitian Hamiltonian [1]

$$H = H_0 - i\gamma H_1, \quad (1)$$

where  $H_0$  is the Hermitian Hamiltonian describing a closed quantum system. The Hermitian  $H_1$  stands for the interaction between the system and the environment. The parameter  $\gamma$  characterizes the strength of the interaction, i.e. the larger  $\gamma$  the larger opening. Usually the Hamiltonian (1) has been studied in terms of the eigenstates of  $H_0$  since  $H_1$  is considered as small perturbation [5, 6]. In this work we instead use the eigenstates of  $H_1$  as bases because we are interested in the opposite limit. Diagonalizing  $H_1$ , Eq. (1) is rewritten as

$$H' = H'_0 - i\gamma H'_1 \quad (2)$$

$$= \begin{pmatrix} \epsilon_1 & c_{12} & \cdots & c_{1N} \\ c_{12}^* & \epsilon_2 & \cdots & c_{2N} \\ \vdots & \vdots & \ddots & \vdots \\ c_{1N}^* & c_{2N}^* & \cdots & \epsilon_N \end{pmatrix} - i\gamma \begin{pmatrix} \Gamma'_1 & 0 & \cdots & 0 \\ 0 & \Gamma'_2 & \cdots & 0 \\ \vdots & \vdots & \ddots & \vdots \\ 0 & 0 & \cdots & \Gamma'_N \end{pmatrix},$$

where  $\Gamma_j (= \gamma\Gamma'_j)$  is the decay rate or the inverse lifetime of the  $j$ th basis state. It is obvious that if the opening is large enough so as to be  $\Gamma_j \gg |c_{jk}|$  all the eigenstates of  $H'$  are almost equivalent to those of  $H'_1$ . One can interpret it to mean that the eigenstates of  $H'$  become *localized* on those of  $H'_1$ . Before discussing what the nature of the eigenstates of  $H'_1$  is, let us consider the simplest case of Eq. (2) with  $N = 2$ , i.e.  $2 \times 2$  matrix model in detail. It provides more precise criteria on the opening-induced localization roughly explained here.

The  $2 \times 2$  matrix model has been widely used for studying two interacting modes of open quantum systems to successfully explain various related experimental and theoretical phenomena [6, 8, 26, 27]. It also exhibits a non-trivial degeneracy known as the EP. Although the parametric evolution of both the eigenvalues and the eigenstates around an EP, as shown in Fig. 1(a) and (b), are now well understood, it has been overlooked how the EP is associated with the localization of the eigenstates.

Assuming non-zero  $c_{12}$  is real for simplicity, the eigenvalues are  $\lambda_{\pm} = (\epsilon_1 + \epsilon_2 - i(\Gamma_1 + \Gamma_2) \pm c\sqrt{\square})/2$  and the corresponding non-normalized eigenstates are

$$\begin{pmatrix} \frac{1}{2} \left( -\frac{\Delta\epsilon}{c} + i\frac{\Delta\Gamma}{c} \pm \sqrt{\square} \right) \\ 1 \end{pmatrix}, \quad (3)$$

where  $\square = \left(\frac{\Delta\epsilon}{c}\right)^2 - \left(\frac{\Delta\Gamma}{c}\right)^2 + 4 - 2i\frac{\Delta\epsilon\Delta\Gamma}{c^2}$ . We set  $\Delta\epsilon = \epsilon_2 - \epsilon_1$ ,  $\Delta\Gamma = \Gamma_2 - \Gamma_1$ , and  $c_{12} = c$ , respectively. The EP occurs at  $(\frac{\Delta\epsilon}{c}, \frac{\Delta\Gamma}{c}) = (0, \pm 2)$ . At  $\Delta\epsilon = 0$ , the eigenstates of Eq. (3) give rise to  $\frac{1}{\sqrt{2}}(\pm 1, 1)^T$  representing the perfectly delocalized—in the sense that it appears to be uniformly distributed over two bases—state for  $|\frac{\Delta\Gamma}{c}| \ll 2$ , while  $(i, 0)^T$  and  $(0, 1)^T$  representing the perfectly localized state for  $|\frac{\Delta\Gamma}{c}| \gg 2$ . It implies that the EP plays a role of the border between localization and delocalization at least in this model.

In order to quantitatively study the localization of the eigenstates, we define the delocalization factor  $F$  as  $(1 - R)/R$  with  $R = \max(|a_1|^2, |a_2|^2)$  when the normalized eigenstate is written as  $(a_1, a_2)^T$ . The perfect localization and the perfect delocalization occur at  $F = 0$  and  $F = 1$ , respectively. Figure 1(c) shows the delocalization factor  $F$  around the EP occurring at  $(0, 2)$ . Only for convenience we choose  $F = 0.5$  as the border between the localized and delocalized states to obtain Fig. 1(d). If the system is closed, i.e.  $\Gamma_1 = \Gamma_2 = 0$ , however, it is shown from Eq. (3) that the eigenstates are delocalized for  $|\Delta\epsilon| \ll |c|$ , while localized for  $|\Delta\epsilon| \gg |c|$ . Once the system is opened,  $\Delta\Gamma$  should be additionally taken into

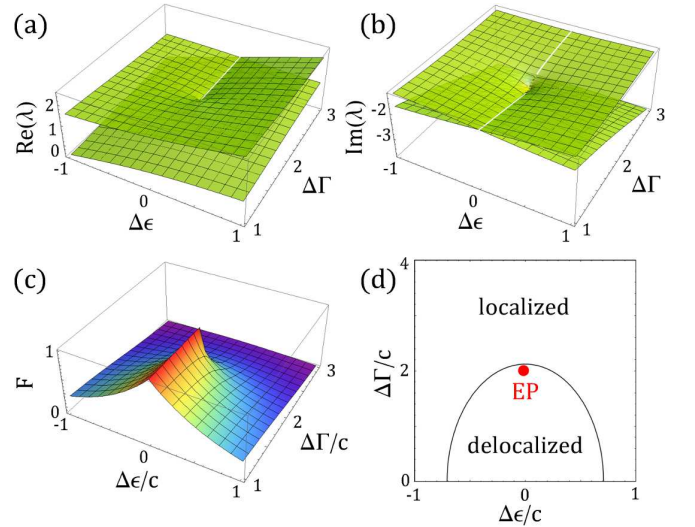


FIG. 1: (color online). (a) The real and (b) the imaginary parts of eigenvalues of  $2 \times 2$  matrix obtained from Eq. (2) with  $N = 2$  when  $\epsilon_1 = \Gamma_1 = c = 1$ . For a given  $\Delta\epsilon$  and  $\Delta\Gamma$  there exist two eigenvalues. (c) The delocalization factor  $F$  in terms of  $\frac{\Delta\epsilon}{c}$  and  $\frac{\Delta\Gamma}{c}$ . (d) The delocalized and the localized region when  $F_c = 0.5$  is chosen.

account; Even if  $|\Delta\epsilon|$  is small enough so as to be delocalized in the closed system, with  $|\Delta\Gamma| \gg 2|c|$  the state appears to be localized.

Prominent feature of Fig. 1(d) is that the range of  $\Delta\epsilon$  where the state is delocalized decreases as  $|\Delta\Gamma|$  increases, and for  $|\Delta\Gamma/c| \gtrsim 2$  all the states are localized irrespective of  $\Delta\epsilon$ . It leads us to conclude that any delocalized state is transformed into a localized state as the opening increases because generally speaking the larger the opening, the larger  $\Delta\Gamma$ . However, it is emphasized that it is not  $\Gamma_1$  and  $\Gamma_2$  but the difference between them to induce localization.

Now let us consider a  $N \times N$  Hamiltonian, i.e.  $H'$  of Eq.(2), where we find many EP's, which formally amounts to the number of choosing a pair among  $N$  distinct modes. It has been found [28] that the complicated properties of whole EP's can be understood by considering individual EP separately. It allows us to directly apply the argument of  $2 \times 2$  matrix model to  $N \times N$  Hamiltonian; When the opening is large enough, each state becomes localized. The  $H'$  describing chaotic systems is easily constructed, in the spirit of the RMT, by choosing the random numbers satisfying  $-1 < \epsilon_j < 1$ ,  $-c < c_{jk} < c$ , and  $0 < \Gamma_j < \gamma$ . It is thus controlled simply by two parameters,  $c$  and  $\gamma$ ; The larger  $c$ , the more chaotic the system. The larger  $\gamma$ , the bigger the opening. Below we numerically show the main feature of localization of the eigenstates observed in the  $2 \times 2$  matrix model is also observed in the  $H'$  with  $N = 3000$ .

To measure the degree of localization of the eigen-

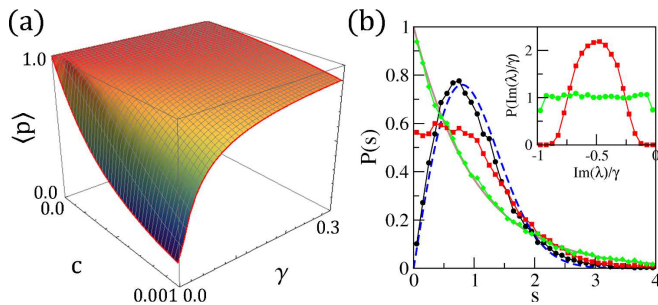


FIG. 2: (color online). (a) The AIPR  $\langle P \rangle$  in terms of  $c$  and  $\gamma$ . The distributions of (b) the level spacings of the real parts of eigenvalues and (Inset) the normalized imaginary parts of eigenvalues at  $\gamma = 0.0$  (black dots),  $0.004$  (red rectangles), and  $0.1$  (green diamonds), respectively, with  $c = 0.001$ . Note that there are no black dots in Inset because no imaginary parts of eigenvalues exist with  $\gamma = 0.0$ . The blue dashed and the brown curves represent the Wigner and the Poisson distributions, respectively.

states of  $H'$ , we introduce the average inverse participation ratio (AIPR), defined as  $\langle P \rangle = \sum_i \left[ \frac{\sum_j |a_j^i|^4}{(\sum_j |a_j^i|^2)^2} \right] / N$  ( $1/N \leq \langle P \rangle \leq 1$ ) where  $a_j^i$  is the  $j$ th element of the  $i$ th eigenstate [29, 30]. The larger  $\langle P \rangle$ , the more strongly localized the state. Figure 2(a) presents the AIPR in terms of  $c$  and  $\gamma$ . When the system is closed, i.e.  $\gamma = 0$ , the AIPR monotonically decreases so that the eigenstates become delocalized as  $c$  increases. However, if the system is open, for a given  $c$  the AIPR monotonically increases to approach one so that the eigenstates become localized as  $\gamma$  increases as shown in Fig. 2(a). This is exactly what we found in  $2 \times 2$  matrix model; Most eigenstates are localized if the opening ( $\gamma$ ) is sufficiently larger than the coupling ( $c$ ). Note that different from Fig. 1(d) the EP is not clearly revealed in Fig. 2(a) since here a lot of EPs are simultaneously involved so that one can see only their overall influence rather than individual contribution. The main message of the matrix model is that *the opening induces localization*.

The transition from the delocalization to the localization of eigenstates influences their statistical properties. As far as the closed system ( $\gamma = 0$ ) is concerned, it is well-known that the level spacing distribution evolves from Poisson to Wigner distributions as  $c$  increases from zero. It is shown in Fig. 2(b) that with  $c=0.001$  fixed the level spacing distribution of the real parts of eigenvalues evolves from the Wigner ( $\gamma = 0$ ) to the Poisson ( $\gamma = 0.1$ ) as  $\gamma$  increases. The localization of the eigenstates generally reduces the overlap between two neighboring eigenstates so as to allow them to closely approach each other. It thus decreases the width of avoided level crossing among them causing the level spacing distribution to change from the Wigner to the Poisson. One remark is that in open systems this is not a whole story.

Even if no localization takes place the real parts of two neighboring eigenvalues can closely approach each other if the imaginary parts of the eigenvalues differ enough. Therefore, the localization itself is a merely necessary condition for the transition from the Wigner to the Poisson. Note that for rather smaller opening ( $\gamma = 0.004$ ), the intermediate distribution represented by the red rectangles of Fig. 2(b) is obtained. The distribution of imaginary parts of eigenvalues is also changed from narrow to wide one as shown in the inset of Fig. 2(b). This can be easily understood since for large enough  $\gamma$  the set of imaginary parts of eigenvalues are simply recover  $\Gamma_j$  chosen randomly.

So far we have shown that large enough opening induces the localization of the eigenstates of  $H'$  on the eigenstates of  $H_1$ . Even though this has already answered the question, why most modes are found to be localized in open quantum systems with classically chaotic dynamics, it is still unclear what the eigenstates of  $H_1$  look like. To get some idea, we need to study a physical example. It also confirms that our results obtained from simple abstract matrix model is valid in a real physical system, e.g. a dielectric microcavity [31, 32].

Before considering the modes of the microcavity in detail, we provide some insight of what the eigenstates of  $H_1$  look like in the microcavity based upon semiclassical argument. As far as the corresponding classical dynamics is concerned, large opening prohibits long time dynamics since the time evolution of a ray is terminated once it touches the opening [33]. It makes only short time dynamics, dominated by unstable manifolds of periodic orbits, relevant. One thus assumes that the eigenstates of  $H_1$  is predominantly described by unstable manifolds, in other words scar-like structures. In fact, it has been found that the direction of far-field outgoing from the chaotic microcavities are determined from the geometry of unstable manifolds [34–36]. Therefore, we expect that for large opening the modes of chaotic microcavities are localized on the short periodic orbits and the associated unstable manifolds. Note that it has been shown that the eigenstates of an open quantum map are localized on the corresponding classical repeller so as to reveal fractal structure [37–39]. The repeller is nothing but collection of unstable manifolds in microcavities.

The resonances and the corresponding modes of a microcavity are obtained from solving the Helmholtz equation,  $[\nabla^2 + n^2(\mathbf{r})k^2]\psi = 0$ , where  $n$  is the refractive index of the dielectric exploited, by using the boundary element method [40]. We focus on TM polarization where both the wavefunction  $\psi$  and its normal derivative  $\partial_\nu \psi$  are continuous across the boundary. The  $\psi$  corresponds to the  $z$  component of the electric field  $E_z$  when the cylindrical symmetry of the cavity is assumed so that it is enough to take the cross sectional area, namely  $xy$ -plane, into account to describe the  $\psi$  [41]. Here we consider the dielectric cavity whose boundary is given as Bunimovich

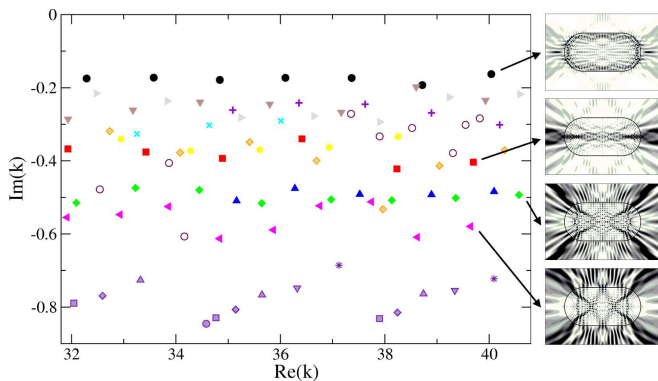


FIG. 3: (color online). The complex eigenvalues of the modes of the stadium-shaped microcavity with  $n = 1.45$ . The modes are grouped by the periodic orbits supporting their intensity pattern in coordinate space; the rectangle (black dots), the arrowhead (brown triangle down and grey triangle right), the diamond (violet plus and cyan x), the triangle (yellow star), the horizontal bouncing ball (red square), the fish (orange shaded diamond), the bowtie (blue triangle up and green diamond), and the candy (magenta triangle left) shaped periodic orbits. The several dots with indigo colors in low Q-region ( $\text{Im}(k) < -0.65$ ) represent the localized modes supported by the bouncing ball type orbits. The maroon open dots represent delocalized or unclassified modes. Four typical localized modes are presented in the right column in grayscale; the rectangular, the horizontal bouncing ball, the bowtie, and the candy shaped orbits from the top.

stadium consisting of a square and two semicircles with radius  $R$ . This is a paradigm model of quantum chaos [42]. Here we set  $R = 1$ . Due to the reflection symmetries with respect to both  $x$  and  $y$  axes, we consider the modes with only even-even parity without loss of generality. Figure 3 shows the real and the imaginary parts of eigenvalues of the modes obtained numerically for  $n = 1.45$ .

It is not easy to directly quantify the localization of statistically meaningful number of modes of the microcavities since it requires enormous numerical effort. Instead, we show that for a given range of eigenvalues almost every modes are localized on the short periodic orbits. Figure 3 shows several sets of localized modes grouped by, if any, the corresponding periodic orbits. The highest-Q modes (black dots), for instance, are localized on the rectangular periodic orbit. Starting from the left ( $k = 32.289 - i0.175$ ) the number of nodes of the spatial wavefunctions of these modes increase from 22 to 28 in the quarter-stadium, from which one obtains the average  $\langle \Delta k \rangle$  is 1.292, where  $\Delta k$  is the spacing between the real parts of eigenvalues of two successive modes. This is well fitted with 1.301 expected from quantization of the path length  $l$  of the rectangular periodic orbit,  $\Delta k^* = 4\pi/l$ . One finds that the spacing  $\Delta k$  is almost equidistant since the difference  $\alpha = |(\langle \Delta k \rangle - \Delta k^*)/\Delta k^*|$

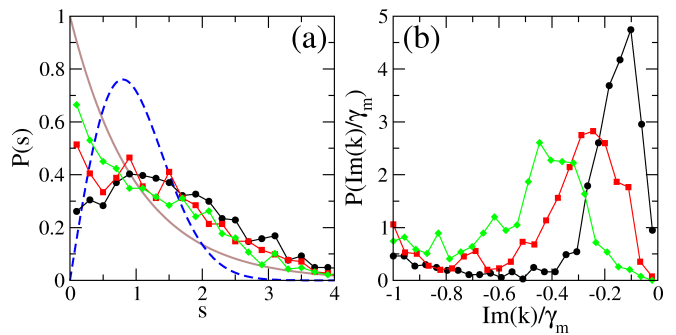


FIG. 4: (color online). The distributions of (a) the level spacing of the real parts of eigenvalues and (b) the normalized imaginary parts of eigenvalues of the stadium shaped microcavities with  $n = 3.3$  (black circles), 2.0 (red rectangles), and 1.45 (green diamonds), respectively. The blue dashed and the brown curves represent the Wigner and Poisson distributions, respectively.

is 0.007 and the standard deviation of  $\Delta k$  is 0.038 (see Table I). It implies that the modes are strongly localized on the rectangular periodic orbit.

Besides the highest-Q modes, most of the modes in Fig. 3 are also localized on the short periodic orbits as summarized in Table I. Note that both  $\alpha$  and  $\sigma$  of all the modes are small enough to prove the equidistant spacing. The group D has a rather larger  $\alpha$  with small  $\sigma$ , where the intensity of the wavefunction appears to be slightly deviated from the corresponding exact periodic orbit, namely a diamond shape. In fact, the diamond periodic orbit is located just above the critical angle, in which it is known that such a deviation, often resulting in the so-called quasiscar, can occur [43]. For low-Q ( $\text{Im}(k) < -0.65$ ), the modes are still found to be strongly localized on the so-called bouncing ball trajectories which form marginally stable orbits to be separated from the other parts of phase space.

Finally we consider the statistics of the eigenvalues of the modes. Figure 4(a) shows the level spacing statistics of the stadium shaped microcavity with three different refractive indices. As the opening becomes larger ( $n$  becomes smaller), the level spacing distribution of  $\text{Re}(k)$ 's evolves from the Wigner to Poisson distribution [Fig. 4(a)], and the distribution of  $\text{Im}(k)$ 's becomes wider [Fig. 4(b)]. This is exactly what we observed in the matrix model.

In summary, we have shown that by using non-Hermitian random matrices large enough opening induces localization, which is also closely associated with the EP. It provides us with a plausible explanation on why most modes are localized in open quantum systems with classically chaotic dynamics. We have also confirmed our expectation by investigating the eigenmodes of the Bunimovich stadium-shaped microcavity with low refractive index. We hope our finding gives some physical

TABLE I:  $\langle \Delta k \rangle$ ,  $\Delta k^*$ ,  $\alpha$ , and  $\sigma$  of each group of the modes shown in Fig. 3 are presented with abbreviation; rectangle (R), arrowhead (A and A2), diamond (D and D2), triangle (T), horizontal bouncing ball (HBB), fish (F), bowtie (B and B2), and candy (C).

	R	A	A2	D	D2	T	HBB	F	B	B2	C
$\langle \Delta k \rangle$	1.292	1.332	1.352	1.278	1.379	1.326	1.553	1.261	1.233	1.211	0.966
$\Delta k^*$	1.301	1.360	1.360	1.405	1.405	1.400	1.571	1.364	1.209	1.209	0.952
$\alpha$	0.007	0.021	0.006	0.090	0.019	0.053	0.011	0.076	0.020	0.002	0.015
$\sigma$	0.038	0.067	0.054	0.018	0.013	0.005	0.152	0.095	0.107	0.061	0.060

insight to understand various properties of open quantum systems such as resonance trapping [1, 44] and physics of PT symmetric systems [45–47].

We thank M. Choi, I. Kim, D. Lippolis, and S.-Y. Lee for discussions. This research was supported by Basic Science Research Program through the National Research Foundation of Korea (NRF) funded by the Ministry of Education (No.2009-0087261 and No.2012R1A1A4A01013955).

---

\* Electronic address: swkim0412@pusan.ac.kr

- [1] I. Rotter, *J. Phys. A: Math. Theor.* **42**, 153001 (2009), and references therein.
- [2] N. Moiseyev, *Non-Hermitian Quantum Mechanics* (Cambridge University Press, Cambridge, UK, 2011).
- [3] T. Kato, *Perturbation Theory of Linear Operators* (Springer, Berlin, 1966).
- [4] W.D. Heiss, *Eur. Phys. J. D* **7**, 1 (1999).
- [5] W.D. Heiss, *Phys. Rev. E* **61**, 929 (2000).
- [6] C. Dembowski, H.-D. Gräf, H.L. Harney, A. Heine, W.D. Heiss, H. Rehfeld, and A. Richter, *Phys. Rev. Lett.* **86**, 787 (2001).
- [7] B. Dietz, H.L. Harney, O.N. Kirillov, M. Miski-Oglu, A. Richter, and F. Schäfer, *Phys. Rev. Lett.* **106**, 150403 (2011).
- [8] S.-B. Lee, J. Yang, S. Moon, S.-Y. Lee, J.-B. Shim, S.W. Kim, J.-H. Lee, and K. An, *Phys. Rev. A* **80**, 011802(R) (2009).
- [9] W.D. Heiss, *J. Phys. A: Math. Theor.* **45**, 444016 (2012).
- [10] H.-J. Stöckmann, *Quantum Chaos, An Introduction* (Cambridge University Press, Cambridge, U.K., 1999).
- [11] O. Bohigas, M.J. Giannoni, and C. Schmit, *Phys. Rev. Lett.* **52**, 1 (1984).
- [12] M.V. Berry, *J. Phys. A* **10**, 2083 (1977).
- [13] A. Voros, in *Stochastic Behaviour in Classical and Quantum Hamiltonian Systems*, edited by G. Casati and G. Ford, Lecture Notes in Physics Vol. 93 (Springer, Berlin, 1979).
- [14] E.J. Heller, *Phys. Rev. Lett.* **53**, 1515 (1984).
- [15] E.B. Bogomolny, *Physica D* **31**, 169 (1988).
- [16] E.J. Heller, in *Chaos and Quantum Physics*, Proceedings of the Les Houches Summer School, Session LII, edited by M.-J. Giannoni, A. Voros, and J. Zinn-Justin (Elsevier North-Holland, Amsterdam, 1991).
- [17] C. Gmachl, E.E. Narimanov, F. Capasso, J.N. Bailargeon, and A.Y. Cho, *Opt. Lett.* **27**, 824 (2002).
- [18] S.-B. Lee, J.-H. Lee, J.-S. Chang, H.-J. Moon, S.W. Kim, and K. An, *Phys. Rev. Lett.* **88**, 033903 (2002).
- [19] T. Harayama, T. Fukushima, P. Davis, P.O. Vaccaro, T. Miyasaka, T. Nishimura, and T. Aida, *Phys. Rev. E* **67**, 015207(R) (2003).
- [20] W. Fang, H. Cao, and G.S. Solomon, *Appl. Phys. Lett.* **90**, 081108 (2007).
- [21] M. Lebental, J.S. Lauret, R. Hierle, and J. Zyss, *Appl. Phys. Lett.* **88**, 031108 (2006).
- [22] W. Fang and H. Cao, *Appl. Phys. Lett.* **91**, 041108 (2007).
- [23] N. Djellali, I. Gozhyk, D. Owens, S. Lozenko, M. Lebental, J. Lautru, C. Ulysse, B. Kippelen, and J. Zyss, *Appl. Phys. Lett.* **95**, 101108 (2009).
- [24] E. Bogomolny, N. Djellali, R. Dubertrand, I. Gozhyk, M. Lebental, C. Schmit, C. Ulysse, and J. Zyss, *Phys. Rev. E* **83**, 036208 (2011).
- [25] S. Bittner, B. Dietz, R. Dubertrand, J. Isensee, M. Miski-Oglu, and A. Richter, *Phys. Rev. E* **85**, 056203 (2012).
- [26] C. Dembowski, B. Dietz, H.-D. Gräf, H.L. Harney, A. Heine, W.D. Heiss, and A. Richter, *Phys. Rev. Lett.* **90**, 034101 (2003).
- [27] J. Wiersig, *Phys. Rev. Lett.* **97**, 253901 (2006).
- [28] J.-W. Ryu, S.-Y. Lee, and S.W. Kim, *Phys. Rev. A* **85**, 042101 (2012).
- [29] L. Kaplan and E.J. Heller, *Ann. Phys.* **264**, 171 (1998).
- [30] L. Kaplan and E.J. Heller, *Physica D* **121**, 1 (1998).
- [31] Edited by R. K. Chang and A. J. Campillo, *Optical Processes in Microcavities* (World Scientific, Singapore, 1996).
- [32] K.J. Vahala, *Nature* **424**, 839 (2003).
- [33] This is somewhat exaggerated because only a part of the rays touching the opening, determined from the Fresnel coefficients, escapes from the cavity, but the key idea here is not influenced by such details.
- [34] H.G.L. Schwefel, N.B. Rex, H.E. Tureci, R.K. Chang, A.D. Stone, T. Ben-Messaoud, and J. Zyss, *J. Opt. Soc. Am. B* **21**, 923 (2004).
- [35] S.-Y. Lee, J.-W. Ryu, T.-Y. Kwon, S. Rim, and C.-M. Kim, *Phys. Rev. A* **72**, 061801(R) (2005).
- [36] S.-B. Lee, J. Yang, S. Moon, J.-H. Lee, K. An, J.-B. Shim, H.-W. Lee, and S.W. Kim, *Phys. Rev. A* **75**, 011802(R) (2007).
- [37] G. Casati, G. Maspero, and D.L. Shepelyansky, *Physica D* **131**, 311 (1999).
- [38] D. Wisniacki and G.G. Carlo, *Phys. Rev. E* **77**, 045201(R) (2008).
- [39] L. Ermann, G.G. Carlo, and M. Saraceno, *Phys. Rev. Lett.* **103**, 054102 (2009).
- [40] J. Wiersig, *J. Opt. A* **5**, 53 (2003).
- [41] J.D. Jackson, *Classical Electrodynamics* (John Wiley and Sons, New York, 1962).

- [42] L. Bunimovich, *Commun. Math. Phys.* **65**, 295 (1979).
- [43] S.-Y. Lee, S. Rim, J.-W. Ryu, T.-Y. Kwon, M. Choi, and C.-M. Kim, *Phys. Rev. Lett.* **93**, 164102 (2004).
- [44] D. Lippolis (private communication).
- [45] C.M. Bender and S. Boettcher, *Phys. Rev. Lett.* **80**, 5243 (1998).
- [46] A. Guo, G.J. Salamo, D. Duchesne, R. Morandotti, M. Volatier-Ravat, V. Aimez, G.A. Siviloglou, and D.N. Christodoulides, *Phys. Rev. Lett.* **103**, 093902 (2009).
- [47] C.E. Rüter, K.G. Makris, R. El-Ganainy, D.N. Christodoulides, M. Segev, and D. Kip, *Nat. Phys.* **6** 192 (2010).